*Quantum Electronics* **48** (8) 767 – 772 (2018)


***COHERENT OPTICAL COMMUNICATION***

https://doi.org/10.1070/QEL16685

# Experimental investigation of nonlinear operation mode of a DP-QPSK 100G link with co-propagating-pump Raman amplification

D.D. Starykh, I.I. Shikhaliev, V.A. Konyshev, O.E. Nanii, V.N. Treshchikov, R.R. Ubaydullaev, D.R. Kharasov

*Abstract.* **The nonlinear interference noise in a coherent single-span fibre-optic communication link (FOCL) with co-propagating Raman amplification is investigated at different levels of input Raman pump and channel powers and dispersion. A simple phenomenological expression for calculating the nonlinear noise power at the output of a single-channel FOCL is presented. The merit of using a distributed Raman amplifier with co-propagating pump up to 1 W in a single-span single-channel FOCL is experimentally investigated.**

***Keywords:*** *distributed Raman amplifier, co-propagating Raman pump, high-speed coherent communication link, 100 Gbit s$^{-1}$, chromatic dispersion, nonlinear interference noise, nonlinear noise accumulation, optical signal-to-noise ratio.*

## 1. Introduction

The most widespread and energetically efficient tool for long-range high-speed data transfer is coherent optical communication [1 – 10]. The maximum operation length and single span length in coherent fibre-optic communication links (FOCLs) are limited mainly by two factors: noise of spontaneous luminescence in the erbium-doped fibre amplifier (EDFA) and the nonlinear effects in fibre. Both these factors reduce the optical signal-to-noise ratio (OSNR) at the transponder receiver input, which leads to degradation of optical signal quality and, as a consequence, to signal demodulation errors. The OSNR in the end line can be improved by increasing the signal power; however, this increase induces nonlinear effects: self-phase modulation, phase cross-modulation, four-wave mixing, etc. In the case of coherent data transfer system, the dispersion is compensated for by the transponder when carrying out digital signal processing [11]; hence, one can do without elements of physical compensation for dispersion. Due to this, because of the large accumulated dispersion, we can treat nonlinear effects as an additive Gaussian noise [3, 12]. Thus, the nonlinear effects in coherent FOCLs can be characterised by nonlinear noise power, which is added to the power of erbium amplifier spontaneous luminescence noise. In this case, the power of the nonlinear noise caused by the interaction of pulses in one channel can approximately be described by the expression

$$P_{\rm NL} = \eta (P^{\rm in}_{\rm signal})^3, \tag{1}$$

where $P^{\rm in}_{\rm signal}$ is the input channel power and $\eta$ is the nonlinearity coefficient. The total signal-to-noise ratio ($\rm OSNR_{BER}$), which takes into account the main factors affecting the signal quality and determining the number of errors during signal demodulation can be described by the formula

$$\frac{1}{\rm OSNR_{BER}} = \frac{P_{\rm ASE} + P_{\rm NL}}{P_{\rm signal}} = \frac{1}{\rm OSNR_L} + \frac{1}{\rm OSNR_{NL}}, \tag{2}$$

where $P_{\rm ASE}$ is the noise of amplified spontaneous emission power, $\rm OSNR_L$ is the linear optical signal-to-noise ratio, and $\rm OSNR_{NL}$ is the nonlinear optical signal-to-noise ratio.

To obtain the best FOCL performance , one must, on the one hand, provide a maximally high power at the line output and, on the other hand, avoid a too high channel power, at which nonlinear effects develop. One of the ways to increase the channel power at the line span output without increasing the nonlinear noise power is to use distributed Raman amplifiers. During stimulated Raman scattering (SRS) [13], the telecommunication fibre plays the role of gain medium. Thus, the signal power and the $\rm OSNR_L$ at the FOCL output increase due to a decrease in the erbium-doped fibre preamplifier gain. Under these conditions, it is more difficult to take into account nonlinear impairments. A model of additive Gaussian noise [14] was developed to calculate the nonlinear noise power; however, it is rather difficult to apply it to real FOCLs, because the theoretical expressions are complicated and contain many signal parameters that are difficult to control. In addition, this model is applicable to only channels with a minimum frequency interval and a constant spectral power density (Nyquist WDM). Simplified phenomeno-

**D.D. Starykh, I.I. Shikhaliev, D.R. Kharasov** Scientific and Technical Center T8, ul. Krasnobogatyrskaya 44, stroenie 1, office 826, 107076 Moscow, Russia; Moscow Institute of Physics and Technology (State University), Institutskii per. 9, 141701 Dolgoprudnyi, Moscow region, Russia; e-mail: starykh@phystech.edu;
**V.A. Konyshev** Scientific and Technical Center T8, ul. Krasnobogatyrskaya 44, stroenie 1, office 826, 107076 Moscow, Russia; S.I. Vavilov Institute of History of Natural Science and Technology, Russian Academy of Sciences, Staropanskii per. 1/5, 109012 Moscow, Russia;
**O.E. Nanii** Scientific and Technical Center T8, ul. Krasnobogatyrskaya 44, stroenie 1, office 826, 107076 Moscow, Russia; Faculty of Physics, M.V. Lomonosov Moscow State University, Vorob'evy gory, 119991 Moscow, Russia; Moscow Institute of Physics and Technology (State University), Institutskii per. 9, 141701 Dolgoprudnyi, Moscow region, Russia;
**V.N. Treshchikov, R.R. Ubaydullaev** Scientific and Technical Center T8, ul. Krasnobogatyrskaya 44, stroenie 1, office 826, 107076 Moscow, Russia

Received 21 March 2018; revision received 18 June 2018
*Kvantovaya Elektronika* **48** (8) 767 – 772 (2018)
Translated by Yu.P. Sin'kov

logical models based on experimental data are used in practice.

Simple and efficient phenomenological models (based on techniques of experimental measurement of nonlinearity coefficient $\eta$) have been developed [15] for the case where Raman amplification is absent, and the signal attenuates exponentially. However, since the signal longitudinal power profile (LPP) changes its shape under SRS amplification conditions, new models and experimental techniques should be developed. A calculation model can be elaborated in different ways for distributed Raman amplifiers with co- and counterpropagating pump. Since the signal power at the FOCL output is low, the nonlinear effects on the last kilometers of the fibre channel are weak; therefore, it is necessary to calculate only the signal and spontaneous Kaman scattering noise powers for counterpropagating Raman pump. In the case of copropagating Raman pump, we must take into account the influence of nonlinear effects on OSNR.

In some works devoted to the design of ultralong unrepeated FOCLs [16–20], it was shown that copropagating Raman pump can successfully be used to increase the FOCL span length. However, an analysis of the contribution of this pump to an increase in the operation length and a technique for choosing FOCL parameters were not reported in those studies.

The purpose of this work was to develop a phenomenological model for calculating the nonlinear noise in a single-channel DP-QPSK 100G FOCL with distributed Raman amplifiers, experimentally verify it, and elaborate a technique for measuring the nonlinear noise power in such links. In addition, we experimentally investigated the total merit from the use of a distributed Raman amplifier with co-propagating 1-W pump under the optimal conditions of communication link operation. The shape of channel LPP was estimated from the input pump and signal powers using an experimentally verified MATLAB program, which was applied to solve numerically the system of rate equations describing the SRS amplification in fibres of different types.

## 2. Experimental setup

A schematic of the experimental setup for measuring the optical single-span communication link parameters is shown in Fig. 1. An optical signal from the bit error rate (BER) analyser transmitter with a data transfer rate of 100 Gbit $s^{-1}$ arrives at the client input of 100G transponder. Excess coding for carrying out anticipatory error correction and obtaining functional information is added to the signal in the transponder, after which the total bit rate becomes equal to 120 Gbit $s^{-1}$. Then the optical signal at a wavelength of 1551.72 nm (the 32th channel of standardised ITU-T network) is directed to the tunable dispersion compensation element to control the input dispersion. An erbium-doped fibre amplifier EDFA1 (tuned to the maximum gain mode) was used to amplify the transponder signal. To increase the accuracy of LPP calculation based on the input signal and pump parameters, a multiplexer was mounted behind the EDFA1, which performed filtering spontaneous emission noise of erbium ions. Then the signal is directed to a variable optical attenuator VOA1 and, jointly with pump at wavelengths of 1439 and 1455 nm from the Raman amplifier, arrives at the pump multiplexer, after which 10% total power is transferred (using a coupler) to a calibrated spectrum analyser OSA1 to measure powers at the input of standard telecommunication fibre SSMF (100 km long, with a total attenuation of 18.9 dB). At the fibre output, the signal is amplified by amplifier EDFA2 and, after passing through an attenuator VOA2 and last preamplifier EDFA3 (which serves as a generator of spontaneous emission noise), is directed through a demultiplexer to the transponder receiver.

The optical signal demodulation quality was estimated from the error level in the client traffic on the BER analyser. The minimum $OSNR_L$ value at the transponder receiver input, necessary for arbitrarily error-free signal demodulation, was chosen (by varying VOA3 attenuator decay) for each set of input parameters, such as dispersion and signal and pump powers. This value of linear OSNR will be further referred to as the required OSNR ($OSNR_R$). Since the nonlinear noise spectrum has the same wavelength range as the signal, this noise cannot be detected using an optical spectrum

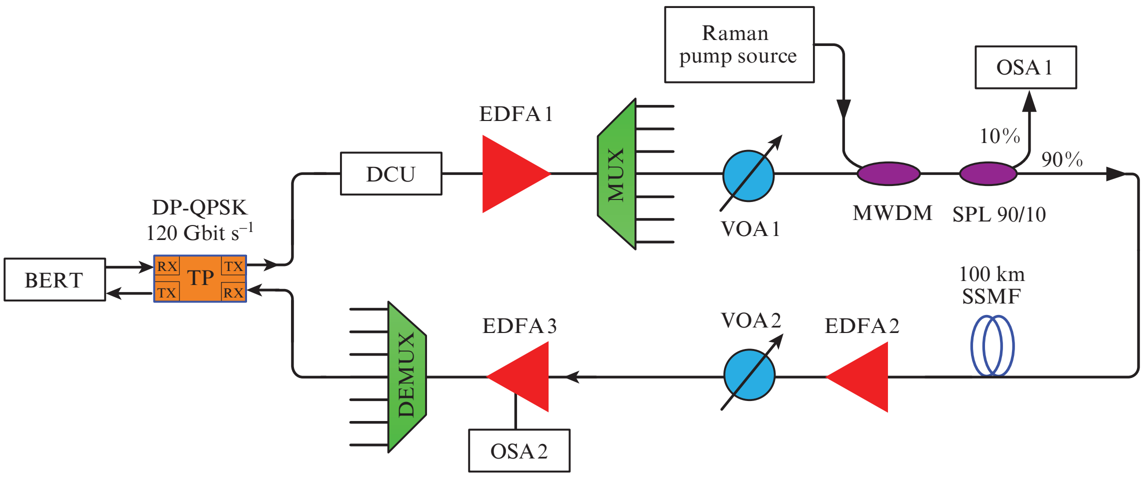


**Figure 1.** Schematic of the experimental setup:
(TP) 100G transponder; (BERT) BER tester; (DCU) variable dispersion compensation unit; (EDFA1–EDFA3) erbium-doped fibre amplifiers; (DEMUX) demultiplexer; (MUX) multiplexer; (VOA1, VOA2) variable optical attenuators; (MWDM) micro-optic wavelength division multiplexer for pumping; (SPL 90/10) optical power splitter with a ratio of 10 : 90; (OSA1, OSA2) optical spectrum analysers; (SSMF) standard single-mode fibre.

analyser. Therefore, its fraction in the total intrachannel noise was estimated indirectly. The required OSNR increases with an increase in the nonlinear noise power, because the linear noise is replaced with nonlinear so as to maintain invariable the $OSNR_{BER}$ value at the transponder input. Thus, the nonlinear OSNR can be found from the formula

$$\frac{1}{OSNR_{NL}} = \frac{1}{OSNR_{BTB}} - \frac{1}{OSNR_{R}}, \quad (3)$$

where $OSNR_{BTB}$ is the required OSNR, measured in the back-to-back scheme, which guarantees absence of nonlinear noise at the transponder receiver input.

## 3. Phenomenological model

When developing a phenomenological model, a question of choosing the input signal and pump parameters (basis for plotting all dependences in future) arose. When Raman pump is performed at different wavelengths, different LPP and nonlinear noise power values correspond to the same input powers. To avoid binding of the developed phenomenological model to a specific type of Raman pump, we associate nonlinear noise power with the LPP shape (Fig. 2).

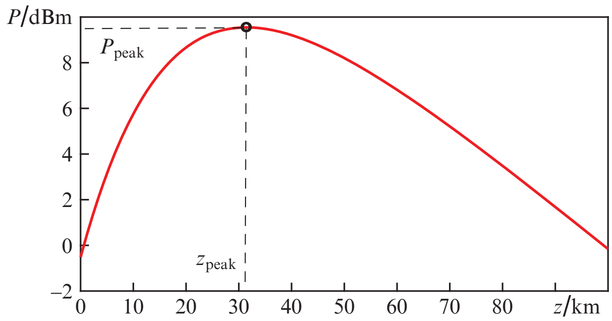


**Figure 2.** Longitudinal profile of channel power $P$ under conditions of copropagating Raman amplification.

Since nonlinear effects arise in the region where the signal power is maximum, it is expedient to describe the LPP by three parameters: maximum channel power ($P_{peak}$), distance of the power peak from the pump input point ($z_{peak}$), and the first derivative $S$ of the function describing the LPP in the vicinity of channel power peak. The latter parameter is necessary in the absence of Raman pump. Thus, using the first two parameters under the Raman pump conditions, one can describe the channel power longitudinal profile by one point with coordinates $z_{peak}$ and $P_{peak}$, as shown in Fig. 2.

## 4. Experimental results

We performed experiments aimed at revealing the dependence of nonlinear noise power on the chosen parameters of channel power longitudinal profile ($z_{peak}$, $P_{peak}$, $S$) and the input dispersion $D_{in}$. It was assumed that the nonlinear noise power at the preamplifier input ($P_{NL}^{out}$) can be written as a product of functions of these parameters:

$$P_{NL}^{out}(z_{peak}, P_{peak}, S, D^{in}) = F_D(D^{in}, z_{peak}) F_S(S) F_z(z_{peak}) F_P(P_{peak}). \quad (4)$$

This hypothesis was further confirmed, and functional dependences on each parameter were found. We analysed the dependence of nonlinear noise power at the output of a 100-km fibre portion on the maximum channel power in the link. To this end, based on the numerical solution of the SRS rate equations, we calculated the input powers of Raman pump and signal that provided constant spatial location of the channel power peak ($z_{peak}$) and variable absolute value of maximum channel power, $P_{peak}$ (Figs 3, 4). A series of such experiments was performed for channel power peaks spaced from the pump input point by 30 and 20 km. It was assumed that, at large values of input dispersion $D_{in}$, the dependence on it levels off, as well as for a coherent FOCL without distributed Raman amplifiers. Therefore, these and subsequent measurements were performed at large input dispersion (–3000 ps nm$^{-1}$) in order to disregard the potentially complex dependence on this parameter in the experiment. The results obtained are presented in Figs 3 and 4. It can be seen in Figs 3b and 4b that the dependences of nonlinear noise power on the maximum channel power are approximated well by a cubic dependence; this circumstance will be further used in the model construction.

Then we investigated the dependence of nonlinear noise power on the distance from the channel power peak to the pump input point ($z_{peak}$). To this end, the input powers of signal and pump were chosen so as to maintain constant the maximum channel power $P_{peak}$ at different pump powers (Fig. 5a). Figure 5b shows one of these dependences. Linear dependences in the form $P_{NL}^{out} \propto (kz_{peak} + 1)$ were obtained for the constant peak channel power $P_{peak}$ = 9.5 dBm, as well for the other $P_{peak}$ values.

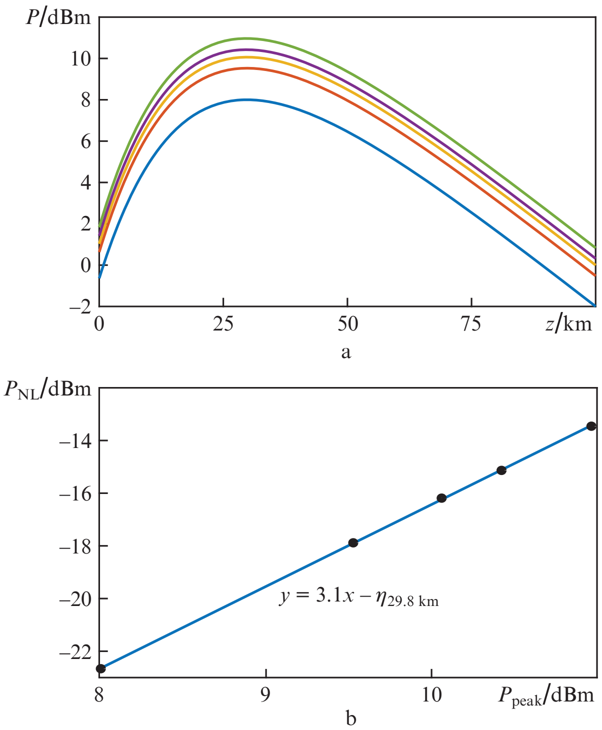


**Figure 3.** (Colour online) (a) Longitudinal channel power profiles and (b) dependence of nonlinear noise power on the maximum channel power in the line for a distance of 29.8 km between the power peak location and the pump input point (circles and solid line are, respectively, experimental values and their approximation).

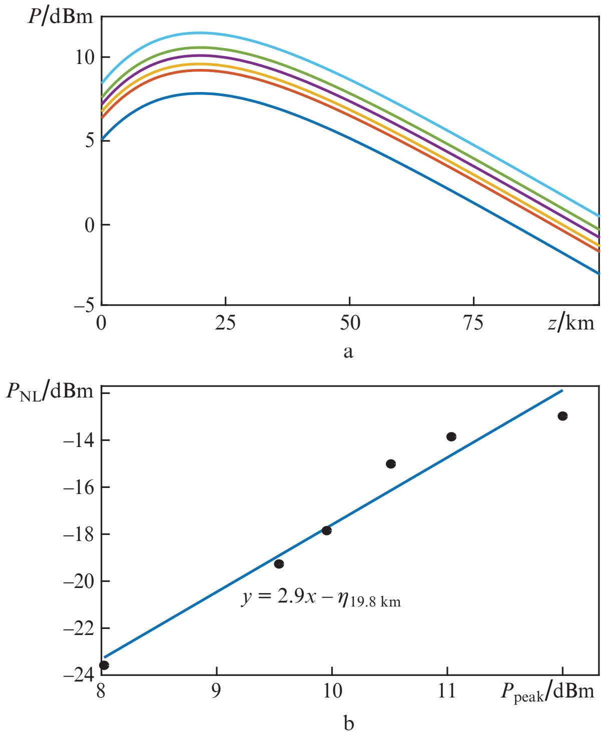


**Figure 4.** (Colour online) (a) Longitudinal channel power profiles and (b) dependence of nonlinear noise power on the maximum channel power in the line for a distance of 19.8 km between the power peak location and the pump input point (circles and solid line are, respectively, experimental values and their approximation).

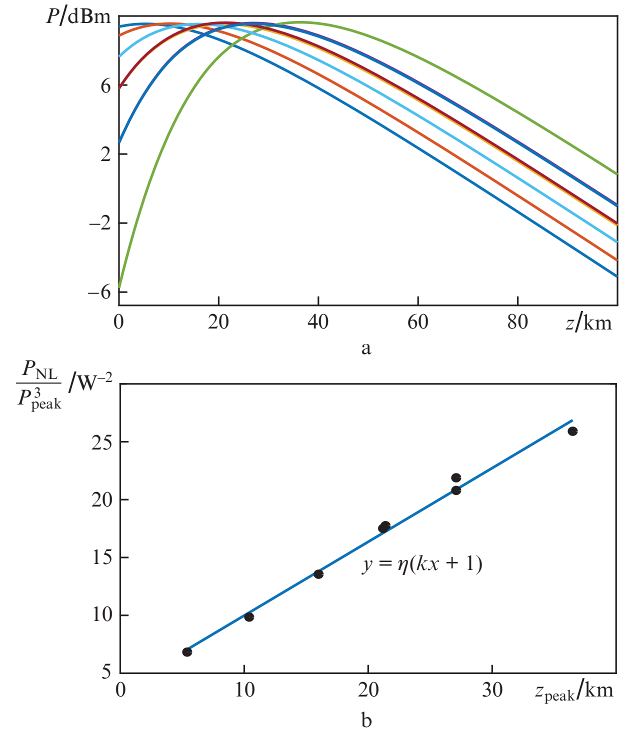


**Figure 5.** (Colour online) (a) Longitudinal channel power profiles and (b) dependence of nonlinear noise power on the spatial location of the channel power peak at $P_{\rm peak}$ = 9.5 dBm: (circles) experimental results and (solid line) their approximation.

The influence of the input dispersion $D_{\rm in}$ on the nonlinear noise power (4) in a FOCL without Raman amplification was described by the approximating formula from [21]:

$$F(D^{\rm in}) = 1 - \exp\left(-\mu_{100} - \left|\frac{D^{\rm in} - D_0}{D_0\rho_0}\right|^{1.5}\right), \qquad (5)$$

where the coefficients $\mu_{100}$, $\rho_0$, and $D_0$ were obtained by approximating the dependence of normalised nonlinear noise power on the input dispersion. The nonlinear noise power at an arbitrary input dispersion was normalised to the nonlinear noise power at large input dispersion (–3000 ps nm$^{-1}$), with other parameters taken fixed.

To expand the range of applicability of formula (5), we assume that the coefficients $\mu_{100}$, $\rho_0$, and $D_0$ depend on the spatial location of channel power peak $z_{\rm peak}$. To verify this assumption, a series of experiments with measuring the dependence of nonlinear noise power on the input dispersion at different locations of channel power peak in the fibre channel was performed (Fig. 6a).

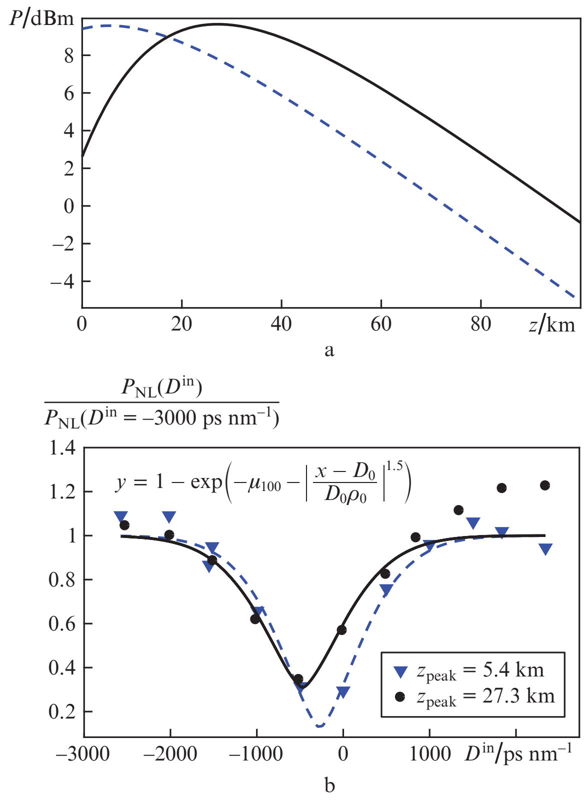


**Figure 6.** (Colour online) (a) Longitudinal channel power profiles and (b) dependences of nonlinear noise power on input dispersion at distances of 5.4 and 27.3 km between the channel power peak location and the pump input point (circles and lines are, respectively, experimental data and their approximations).

Figure 6b shows how the shape of the approximating curve changes with an increase in the distance between the channel power peak and the pump input point. The dependence of each parameter of the approximating function on $z_{\rm peak}$ was described by a polynomial, whose power was chosen proceeding from the best convergence conditions. The final formula can be written as

$$F_D(D^{\text{in}}, z_{\text{peak}}) = 1 - \exp\left(-\mu_{100} - \left|\frac{D^{\text{in}} + D_0 + D_1 z_{\text{peak}} + D_2 z_{\text{peak}}^2}{\rho_0(-D_0 - D_1 z_{\text{peak}} - D_2 z_{\text{peak}}^2)}\right|^{1.5}\right). \quad (6)$$

To calculate the nonlinear noise power under conditions of weak Raman pump, one needs more than one LPP point, because different LPPs correspond to the same $z_{\text{peak}}$ and $P_{\text{peak}}$ values. Due to the Raman amplification, the distance at which the channel power is maintained at a constant level increases with a smooth increase in the pump power (Fig. 7); as a result, the region where nonlinear effects occur is expanded, and the nonlinear noise power at the link output increases. The channel power peak neither changes nor shifts from the beginning of the fibre channel. The first numerical derivative of the function describing the LPP at a point spaced from the channel power peak by 5 km can be used to establish a correspondence between the LPP shape and the related nonlinear noise power.

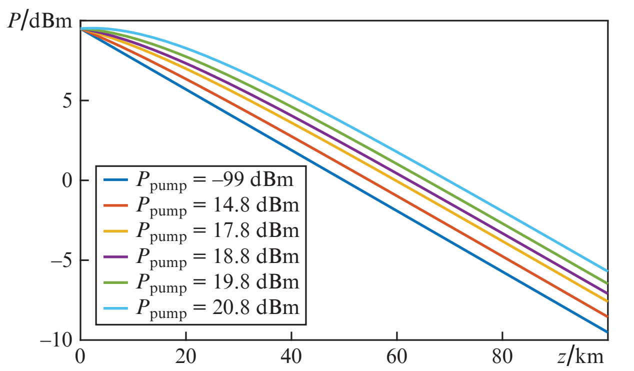


**Figure 7.** (Colour online) Longitudinal channel power profiles at low Raman pump powers $P_{\text{pump}}$.

The transition to the power profile with exponential decay is related to the first derivative $S$ of the function describing the LPP at the point spaced from $z_{\text{peak}}$ by 5 km and is determined by the linear dependence

$$F_S(S) = 2\Theta(-z_{\text{peak}})(b_1 S - b_0) + 1, \quad (7)$$

where $\Theta$ is the Heaviside function; and $b_0$ and $b_1$ are numerically chosen coefficients. The final dependence of the nonlinear noise power on the LPP parameters in the channel has the form

$$P_{\text{NL}}^{\text{out}}(z_{\text{peak}}, P_{\text{peak}}, S, D^{\text{in}}, L_{\text{span}}, \alpha) = \exp[-\alpha(L_{\text{span}} - 100)]$$

$$\times \eta_0\left[1 - \exp\left(-\mu_{100} - \left|\frac{D^{\text{in}} + D_0 + D_1 z_{\text{peak}} + D_2 z_{\text{peak}}^2}{\rho_0(-D_0 - D_1 z_{\text{peak}} - D_2 z_{\text{peak}}^2)}\right|^{1.5}\right)\right]$$

$$\times [2\Theta(-z_{\text{peak}})(b_1 S - b_0) + 1](k z_{\text{peak}} + 1) P_{\text{peak}}^3, \quad (8)$$

where $\eta_0$ is the fundamental nonlinearity coefficient, $L_{\text{span}}$ is the span length (in km), and $\alpha$ is the attenuation in the fibre (in km$^{-1}$).

## 5. Experimental verification of the phenomenological model

One of the main parameters of FOCL reliability is the OSNR margin (in dB), given by the formula

$$\text{osnr}_{\text{M}} = \text{osnr}_{\text{L}} - \text{osnr}_{\text{R}}. \quad (9)$$

The applicability of the proposed phenomenological model for calculating the OSNR margin was analysed by comparing the calculated and experimental results. Three types of Raman amplifiers with pump wavelengths ranging from 1425 to 1480 nm were considered. The input pump power and the signal power were varied in the ranges of 0–1 W and 10 μW–25 mW, respectively; the link lengths were 100 and 150 km. The DP-QPSK 100G modulation format was applied. The difference between the theoretical and experimental results in the entire range under study was shown to be no more than 1 dB. The experimental and calculated results for one of the amplifiers are presented in Fig. 8. In addition, it was demonstrated that the use of a Raman amplifier with co-propagating pump power up to 1 W makes it possible to raise the OSNR$_{\text{BER}}$ value at the transponder receiver input by 6 dB or increase the link span length by about 30 km.

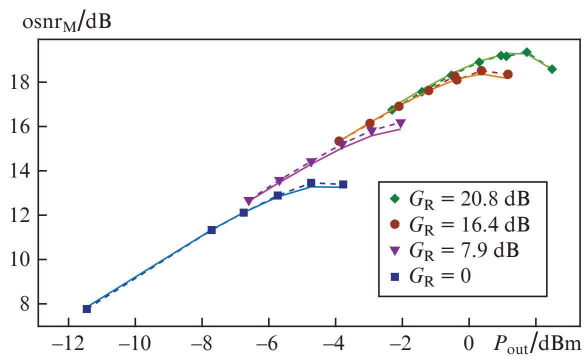


**Figure 8.** (Colour online) Dependences of the OSNR margin on the output channel power $P_{\text{out}}$ at different gains $G_{\text{R}}$ of distributed Raman amplifier with co-propagating pump: (symbols) experimental data and (solid lines) calculation results.

The verification showed that, in the case of communication systems based on the DP-QPSK 100G modulation format, phenomenological model (8) provides calculation of the OSNR margin with an error not larger than 1 dB in an SSMF FOCL span of such a length that the extremum of the function describing LPP is located at a distance of no less than 15 km from the span end. For most of commercially available distributed Raman amplifiers with pump power up to 1 W, the extremum is located at a distance of 10–50 km from the pump input point (depending on the input signal power). When calculating FOCL parts with lengths falling out of the recommended length range, the model yields overestimated values of nonlinear noise power. Thus, the obtained dependences can be recommended to calculate spans of coherent DP-QPSK 100G FOCLs with lengths starting from 65 km and arbitrary input dispersion.

## 6. Conclusions

It was experimentally shown that the nonlinear noise power under conditions of distributed Raman amplification has a cubic dependence on the peak channel power. It was demonstrated that the power of nonlinear interference noise at the FOCL output linearly increases with distance in the position of the channel power peak relative to Raman pump input point. It was found that an increase in distance of the channel power peak relative to Raman pump input point reduced the optimal (with respect to the margin of OSNR) dispersion precompensation. It was also shown that the use of a 1-W co-propagating Raman pump power makes it possible to increase the total OSNR at the link output by 6 dB or increase the length of the single-span line by 30 km. We proposed a simple formula for calculating the nonlinear noise power at the output of a single-channel coherent FOCL containing a distributed Raman amplifier with co-propagating pump. This formula separately takes into account the channel peak power and its position, the Raman pump power, and the input dispersion.

## References


1. Gainov V. et al. *Opt. Express*, **22** (19), 22308 (2014).
2. Gainov V.V. et al. *Laser Phys. Lett*., **10** (7), 75107 (2013).
3. Gurkin N.V., et al. *Quantum Electron*., **43** (6), 550 (2013) [*Kvantovaya Elektron*., **43** (6), 550 (2013)].
4. Chang D. et al. *J. Lightwave Technol*., **33** (3), 631 (2015).
5. Carena A. et al. *J. Lightwave Technol*., **30** (10), 1524 (2012).
6. Konyshev V.A. et al. *Opt. Commun*., **355**, 279 (2015).
7. Poggiolini G.B. et al. *IEEE Photonics Technol. Lett*., **24** (14), 1230 (2012).
8. Konyshev V.A. et al. *Opt. Commun*., **349**, 19 (2015).
9. Poggiolini P. et al. *J. Lightwave Technol*., **32** (4), 694 (2014).
10. Poggiolini P. et al. *IEEE Photonics Technol. Lett*., **23** (11), 742 (2011).
11. Savory S.J. *IEEE J. Sel. Top. Quantum Electron*., **16** (5), 1164 (2010).
12. Poggiolini P. *J. Lightwave Technol*., **30** (24), 3857 (2012).
13. Agrawal G. *Nonlinear Fibre Optics* (New York: Acad. Press, 2001) p. 467.
14. Poggiolini P. et al. https://arxiv.org/ftp/arxiv/papers/1209/1209.0394.pdf.
15. Konyshev V.A., et al. *Quantum Electron*., **46** (12), 1121 (2016) [*Kvantovaya Elektron*., **46** (12), 1121 (2016)].
16. Chang D.I. et al. *Opt. Express*, **19** (26), B971 (2011).
17. Bissessur H. et al. *Proc. European Conf. on Optical Communication (ECOC 2014)* (Cannes, 2014).
18. Chang D.I. et al. *Proc. IEEE Photonics Conf. (IPC 2014)* (San Jose, 2014).
19. Etienne S. et al. *Proc. European Conf. on Optical Communication (ECOC 2015)* (Valencia, 2015).
20. Zhu B. et al. *IEEE Photonics Technol. Lett*., **25** (19), 1863 (2013).
21. Konyshev V.A. et al. *Opt. Commun*., **381**, 352 (2016).